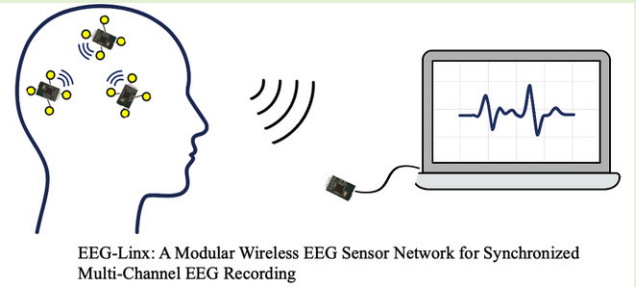
A Wireless, Scalable, and Modular EEG Sensor Network Platform for Unobtrusive Brain Recordings

Ruochen Ding, Charles Hovine, Piet Callemeyn, Michael Kraft, *Member, IEEE*, and Alexander Bertrand, *Senior Member, IEEE*

***Abstract*—This article introduces a modular sensing platform for wearable electroencephalography (EEG) recordings. The platform is conceived as a wireless EEG sensor network (WESN), consisting of multiple miniaturized, wireless EEG sensor nodes that synchronously collect EEG data from different scalp locations. As there are no wires between the different sensors, the platform provides maximal flexibility and discreetness, combined with a reduced sensitivity to motion artifacts or electromagnetic interference. By removing the driven right leg (DRL) electrode and reducing the within node electrode spacing to 3 cm, we obtain a compact design while maintaining a high signal integrity. The WESN system was validated through a series of experiments: achieving synchronization of EEG data transmission across multiple sensor nodes and the detection of actual neural responses in EEG experiments. These results demonstrate the effectiveness and robustness of the proposed WESN platform, establishing it as a promising research platform for scalable, flexible, and discreet multichannel EEG monitoring in ambulatory settings.**



***Index Terms*— Brain–computer interface (BCI), electroencephalography (EEG), wireless EEG sensor network (WESN).**

I. Introduction

ELECTROENCEPHALOGRAPHY (EEG), as a noninvasive method for recording neural signals, gained significant attention in medical research and neuroscience in recent years [1]. The widespread application of EEG has deepened our understanding of brain functions and driven the development of various health-related applications, for example, sleep studies, mental health monitoring, epilepsy, and brain–computer interfaces (BCIs). The use of EEG has expanded from laboratories and hospitals into daily life, particularly in the development of long-term neural monitoring systems and BCIs. For instance, fatigue driving monitoring systems use real-time EEG monitoring to evaluate the driver's cognitive state and prevent traffic accidents [2]. Moreover, EEG is used in the prediction and monitoring of epileptic seizures, helping patients take preventive measures in time to reduce health risks [3], [4]. Applications have also expanded to personalized monitoring in areas such as sleep quality and stress levels, supporting timely health interventions [5], [6]. Other uses include cognitive workload monitoring [7], [8], mobile BCIs [9], and neurosteered hearing devices [10].

The study in [11] provides a detailed overview of the commercial wireless EEG systems that are currently available. Similarly, [12] provides a summary of state-of-the-art wearable EEG sensing technologies, including different electrode types. Despite advancements in signal acquisition quality and user comfort, the existing wireless systems are generally very bulky and therefore stigmatizing. Furthermore, their large size also makes them more susceptible to motion artifacts, wire-pulling artifacts, and electromagnetic artifacts. These conventional EEG setups also rely on centralized data processing, which can lead to issues such as high energy consumption and

Received 29 March 2025; accepted 10 April 2025. Date of publication 25 April 2025; date of current version 16 June 2025. This work was supported by European Research Council (ERC) through European Union's Horizon 2020 Research and Innovation Programme under Grant 802895 and Grant 101138304. The associate editor coordinating the review of this article and approving it for publication was Dr. Yun-Ju Lee. *(Corresponding author: Ruochen Ding.)*

This work involved human subjects or animals in its research. Approval of all ethical and experimental procedures and protocols was granted by the KU Leuven Social and Societal Ethics Committee.

Ruochen Ding, Charles Hovine, Michael Kraft, and Alexander Bertrand are with the Department of Electrical Engineering (ESAT), KU Leuven, 3000 Leuven, Belgium (e-mail: ruochen.ding@kuleuven.be; charles.hovine@kuleuven.be; michael.kraft@kuleuven.be; alexander.bertrand@kuleuven.be).

Piet Callemeyn is with Sentineo, 3001 Leuven, Belgium (e-mail: piet@sentineo.com).

Digital Object Identifier 10.1109/JSEN.2025.3562791

1558-1748 © 2025 IEEE. All rights reserved, including rights for text and data mining, and training of artificial intelligence and similar technologies. Personal use is permitted, but republication/redistribution requires IEEE permission.
See https://www.ieee.org/publications/rights/index.html for more information.
Authorized licensed use limited to: KU Leuven University Library. Downloaded on January 23,2026 at 12:16:33 UTC from IEEE Xplore. Restrictions apply.

increased data transmission latency. These constraints often limit the usability of these systems in dynamic and long-term monitoring scenarios.

As an alternative to head-mounted systems in ear EEG offers more portable and discreet solutions [13]. Recent studies have shown that in ear EEG can effectively support applications like sleep stage analysis and real-time detection of abnormal brain activity, such as seizure patterns, in natural settings [3], [13], [14]. These systems are well suited for long-term monitoring, minimizing visible hardware and providing greater comfort for users. However, their signal recording capabilities can be limited compared to head-mounted systems, especially in terms of spatial resolution and coverage. Other ear-based solutions like the cEEGrid [15], which uses flexible electrode arrays around the ear, have been developed to improve comfort and reduce visibility for extended wear. Nevertheless, all these ear-based setups are limited in the number of channels and spatial coverage of the electrode grid. In addition, they often depend on setups with long wires (e.g., between both ears or to an external amplifier), reducing discreetness and potentially introducing motion or wire artifacts in the recorded signals.

To address these limitations, the concept of the so-called wireless EEG sensor network (WESN) was introduced in [16] as a platform for discreet yet scalable multichannel EEG monitoring. A WESN is conceptualized as a collection of wireless EEG sensor nodes, each equipped with an embedded processor and wireless communication capabilities. The different sensor nodes are galvanically isolated from each other, eliminating physical connections between them to improve discreetness and flexibility in their deployment, and to reduce wire-induced artifacts. Each node is connected to its own local set of electrodes and uses one of these as a local reference electrode, akin to a bipolar montage. Such distributed WESN architectures have been (conceptually) investigated in several EEG signal processing studies in terms of optimal node placement or energy-efficient algorithms for various EEG monitoring tasks [17], [18], [19], [20], [21], [22]. While some research has proposed multiple small sensor nodes, these systems have been predominantly evaluated in network simulators, with limited emphasis on practical hardware implementation and validation in the real world [23].

In this article, we present a first prototype of such a WESN, which we refer to as EEG-Linx, in the form of a modular research platform consisting of miniaturized, wireless EEG sensor nodes that can jointly collect synchronized multichannel EEG activity at various scalp locations. Unlike bulky headset-based commercial EEG systems with fixed electrode configurations, EEG-Linx enables a flexible, multisensor approach with independent sensor placement. While commercial systems may excel in certain hardware metrics (e.g., battery capacity and transmission range), EEG-Linx prioritizes miniaturization, scalability, and modularity.

The EEG-Linx prototype consists of a modular architecture, in which each sensor node operates independently and is equipped with its own microcontroller unit (MCU). The nodes are wirelessly connected to each other and/or to a single node that acts as a data sink. The modular and wireless design allows for flexible node placement, scalability, and customization to meet specific research needs without disrupting overall functionality. Fig. 1 illustrates the EEG-Linx system, showing the conceptual placement of the wireless EEG nodes and the compact hardware design of an individual node.

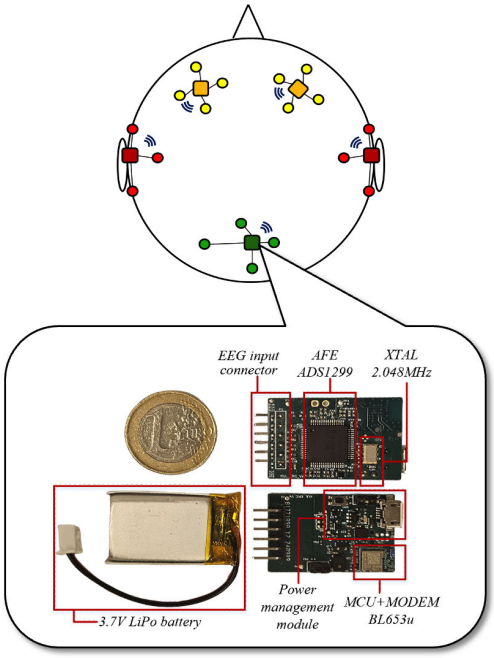


Fig. 1. Conceptual illustration of the EEG-Linx sensor platform (front and back views).

Each EEG sensor node is capable of collecting up to four EEG channels using short wires from the PCB to a few nearby electrodes. To facilitate miniaturization, we have eliminated the need for a driven right leg (DRL) electrode, which is typically placed far away from the recording electrodes. The removal of the DRL is crucial in a WESN platform, as otherwise, each EEG sensor node would require its own separate DRL electrode, thereby introducing many redundant electrodes, which affect the platform's discreetness. We will demonstrate that high-quality EEG signals can be recorded that allow us to detect steady-state neural responses, even in such a miniaturized setup where we limit the within node electrode spacing to 3 cm.

Furthermore, the decentralized structure of our WESN supports real-time monitoring where multiple sensor nodes together collect EEG data that is synchronized across the nodes, thereby facilitating interchannel coherence analysis and multichannel signal processing algorithms [16]. This is demonstrated in an additional experimental setup, showcasing the system's capability to handle data aggregation and maintain synchronization across the network.

This article is organized as follows. Section II further expands on the overall system architecture of our EEG-Linx prototype. Section III presents the firmware platform developed for this system. Section IV details the experimental setup and validation results. Finally, conclusions are drawn in Section V.

Authorized licensed use limited to: KU Leuven University Library. Downloaded on January 23,2026 at 12:16:53 UTC from IEEE Xplore. Restrictions apply.

II. System Description

A. Main Contributions and Key Features of the Platform

The main innovations of our EEG-Linx WESN prototype include as follows.

1) Miniaturized Node Design: The platform uses four-channel sensor nodes, which were designed for compactness, with a double-sided PCB dimension of 2 × 3 cm. The design is further refined by eliminating the need for an additional ground or DRL electrode, which facilitates a compact bipolar setup with a small number of electrodes at each individual node. This implies that a two-channel node only requires three electrodes (typically placed in a right-angle triangular shape to capture all dipole orientations [19]). The sensor nodes have been validated to capture EEG signals with an interelectrode spacing of merely 3 cm, using wet Ag/AgCl electrodes. These design choices ensure effective signal capture within a small form factor, supporting flexible placement on the head and adapting to various brain monitoring scenarios.

2) Modular Architecture: The EEG-Linx platform features a modular design where each sensor node operates independently with its own integrated MCU. One node can function as a "data sink" node, receiving data from other nodes, which increases the system's scalability and adaptability. This architecture allows nodes to be added, replaced, or repositioned without disrupting the entire network, maintaining system reliability even if individual nodes fail or are removed. The resulting scalability and flexibility make the system suitable for a wide range of applications.

3) Wireless Communication: The sensor nodes can wirelessly communicate with each other via a radio operating in the ISM band. This wireless network supports dynamic interaction and real-time adjustments for effective EEG monitoring and data collection. The absence of long wires between the nodes reduces EEG artifacts due to wire pulling, motion, or electromagnetic coupling with other interference sources.

4) Synchronization Across Nodes: Each EEG sensor has its own local clock signal, which introduces a sampling offset and a potential drift between the signals of different nodes. Our platform ensures that the EEG data collected from different nodes are synchronous and accurately aligned in time, by using one of the nodes as the reference clock. This synchronization is important for multichannel or coherence-based analysis, allowing for consistent integration of data from multiple scalp locations; even though the data were collected by galvanically isolated sensors.

These innovative features result in a highly scalable, flexible, and versatile research platform for discreet EEG recordings in mobile or out-of-the-lab setups.

B. System Architecture

Numerous EEG hardware implementations have been developed, ranging from systems using complementary metal–oxide–semiconductor (CMOS) technology for integrated circuits to prototypes built with off-the-shelf discrete components. For instance, the 0.18-μm eight-channel epilepsy control SoC [3] and the 65 nm in ear BCI controller [24] offer benefits like reduced size and low power consumption.

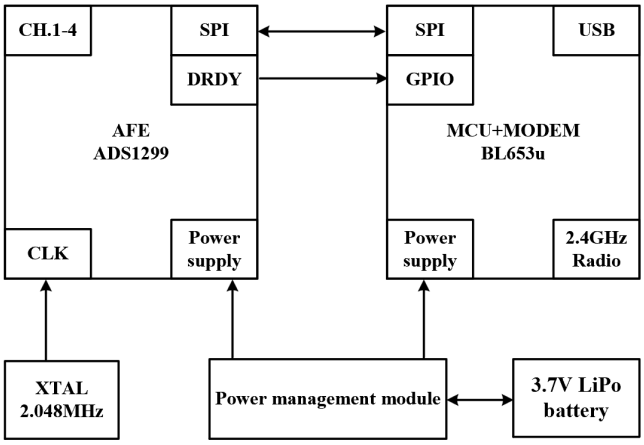


Fig. 2. Hardware architecture of EEG-Linx sensor node.

However, these advantages come with high development costs, long timelines, and limited adaptability. In contrast, systems built with off-the-shelf components, like the 16-channel EEG data acquisition system described in [20] enable faster prototyping and development. Yet, most of these designs tend to be bulkier and often rely on centralized rather than distributed architectures [26], [27], [28], [29].

In our approach, we present an off-the-shelf solution that avoids the large nonrecurring engineering costs and development times associated with custom CMOS chips. Our design features a compact node that includes an analog front end (AFE) for EEG signal acquisition, an MCU with an integrated 2.4-GHz radio for wireless communication, and a power management module. The node is powered by a 3.7-V, 250-mAh LiPo battery. Fig. 2 provides an overview of its hardware architecture.

1) Analog Front End: The AFE of our EEG sensor node employs the ADS1299 chip from Texas Instruments, which is specifically designed for high-resolution EEG signal acquisition [30]. The chip operates with a sampling rate of 250 Hz and is capable of detecting signal amplitudes as low as 10-μV peak, supported by its low input-referred noise of less than 1-μV rms. The ADS1299 communicates signal data to the host via a serial peripheral interface (SPI). A data-ready (DRDY) pin is provided to notify the SPI host when the EEG signal data conversion is complete. In addition, the chip includes programmable gain amplifiers (PGAs) with a maximum gain of 24, which significantly improves the sensitivity of EEG signal acquisition.

The electrodes within a single node are locally configured in a referential montage, where each electrode (e.g., CH1 in Fig. 3) measures EEG signals relative to a local reference electrode (REF). As each node uses its own local reference electrode, a multinode WESN setup would therefore be more akin to a bipolar montage. A common reference montage across nodes would require connecting the REF pins of all nodes to the same electrode, which is possible, but it is not the intended use case in this article. Based on previous studies that have demonstrated the feasibility of a 3-cm spacing between the recording and the REF electrode for capturing relevant

Authorized licensed use limited to: KU Leuven University Library. Downloaded on January 23,2026 at 12:16:53 UTC from IEEE Xplore. Restrictions apply.

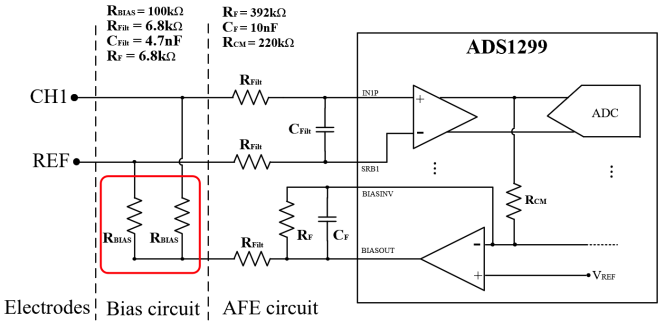


Fig. 3. Simplified AFE circuit with bias resistor configuration for a single EEG channel.

EEG signals [21], [31], [32], we adopted this compact spacing in the validation of our design (see Section IV-B1). Each node in our system supports up to $N = 4$ channels.

The human body can act as an antenna, picking up electromagnetic interference (EMI), particularly from 50-/60-Hz power lines, which results in a common-mode noise on the recorded EEG signals [33]. Despite the TI's ADS1299 very high common-mode rejection ratio (>110 dB), the full systems have a much lower effective CMRR. This is due to the so-called potential divider effect [34], which means that a fraction of the common-mode noise at the electrode inputs is converted into a differential voltage at the amplifier input, which is proportional to the impedance mismatch of the two input electrodes. This problem can be mitigated by the use of an extra bias electrode (often referred to as DRL) that feeds back the common-mode voltage sensed at the amplifier's inputs to the body, therefore attenuating the common-mode noise before it is converted to a differential signal [35], [36]. In addition, this DRL electrode (often combined with the ground electrode) ensures that the amplifier remains within its operational range.

However, since the nodes in our WESN setup are galvanically isolated from each other, such an approach would require an extra electrode for ground and DRL for each individual node, which would hamper the miniaturization and practicality of our system. Therefore, we do not use a separate ground or DRL electrode and instead feedback the common-mode voltage on the device itself, rather than via the body, by connecting it to the electrode pins with bias resistors in between. These resistors are labeled as R_{BIAS} in Fig. 3, which presents a single channel as an example. While this approach does not reduce the part of the common-mode noise that has been converted to differential noise, it will attenuate the remaining fraction of the common-mode noise by reducing the common-mode input impedance seen at the amplifier's inputs [37]. While the relationship between common-mode-noise rejection, common-mode input impedance, and electrode mismatch is rather complicated [37], [38], it has been shown that for moderate impedance mismatches (<20 k) in the inputs, a lower effective common-mode impedance results in a reduced common-mode noise at the amplifier's inputs [37], which motivates this setup. In addition, this active feedback mechanism ensures that the dc common-mode component is as close as possible to the midpoint of the amplifier's input range, which was observed to result in more stable recordings compared to simply omitting the DRL circuit (see Section IV-B2). In this way, an N-channel node requires only $N + 1$ electrodes (one for each channel and one shared reference) instead of $N+2$ when using a ground/DRL electrode. This configuration reduces the number of required electrodes, aligning with our miniaturization goals. If desired, the node can also be set up with an actual DRL electrode, requiring only the removal of the bias resistors.

The selection of the bias resistor values directly affects both input impedance and common-mode noise rejection. Higher resistor values increase input impedance, minimizing the loading effect on the electrodes, thereby preserving the integrity of the EEG signals. On the other hand, lower resistor values result in a lower effective common-mode impedance [37]. In our design, we selected 100-kΩ resistors for the bias circuit. These resistors provide an input impedance ten times higher than the electrode–skin impedance, which is typically maintained below 10 kΩ in EEG recordings. This choice strikes a balance between preventing the attenuation of the EEG signal and maintaining effective noise rejection. We note that, although the introduction of these resistors may contribute some additional thermal noise, their impact is minor as it will fall below the ADS1299's noise floor (<1-μV rms) in standard operating conditions.

2) MCU Module: The BL653u module serves as both the MCU and the wireless communication interface. Measuring only 6.3 mm by 8.6 mm, this module integrates the nRF52833 SoC from Nordic Semiconductor, which was selected for its compact size and powerful capabilities. The nRF52833 features a 32-bit ARM-Cortex-M4 processor with a floating-point unit (FPU) running at 64 MHz. This processor acts as the SPI Controller to retrieve high-resolution EEG data from the ADS1299 chip.

The BL653u's 2.4-GHz radio enables wireless transmission of the processed EEG data to another node acting as a data sink, eliminating the need for physical cables. The BL653u supports a maximum transmit power of +8 dBm, providing strong and stable communication. By centralizing processing, communication, and energy management within a compact footprint, the BL653u module is ideally suited to our WESN system.

3) Power Management Module: The power management module of our EEG sensor nodes employs a single-stage power supply, avoiding the complexity and potential failures associated with multiple power sources. The system is powered by a rechargeable 3.7-V, 250-mAh LiPo battery, measuring 1.8 × 3 cm. The power management system generates all the required digital and analog voltages to the ADC, MCU module, ensuring consistent distribution of power to all components.

Using battery power helps maintain the stability and accuracy of the EEG signals by minimizing noise and interference from external sources. The system also includes a USB charging circuit for convenient recharging directly on the circuit board. In addition, the Micro-USB port can be used as an alternative data transmission channel (for example the data sink node can act as a dongle that is connected to the Micro-USB

Authorized licensed use limited to: KU Leuven University Library. Downloaded on January 23,2026 at 12:16:53 UTC from IEEE Xplore. Restrictions apply.

TABLE I
PARAMETERS OF EEG-LINX SENSOR NODE

Description	Parameter
Dimensions	2cm x 3cm
Number of channels	4
Sampling frequency	250 Hz
Max transmission distance	21m
Consumption	50mA
Power supply	3.7V

port of a smartphone or PC). The power module consists of a 5-V switched-capacitor converter (LM2750SD-5.0), a 3.3-V LDO regulator (AP7331), and a lithium battery charging module (MCP73832T). The LM2750SD-5.0 is a switched-capacitor converter chosen to reduce noise on the supply line and minimize EMI interference. Compared to traditional inductive converters, the switched-capacitor design provides lower noise and better compatibility with sensitive analog components. Decoupling capacitors are placed at each stage to filter out ripple noise, providing a stable power supply.

4) Prototype Characteristics: The prototype of the resulting EEG sensor node is presented in Fig. 1 with an indication of each module. For the PCB design, we adopt a six-layer approach that employs a signal-ground-signal-signal/power-ground-signal stack-up. This structure allows close coupling between the signal layer and power plane with their adjacent ground planes, which helps to minimize noise and enhance signal integrity. Table I presents the characteristics of our EEG sensor node.

III. FIRMWARE PLATFORM

The firmware platform of our EEG sensor node is designed to efficiently manage data acquisition, synchronization, wireless transmission, and data aggregation. Each sensor node operates independently and is identical in hardware, allowing any node to serve as the data sink node when connected to a PC via USB. During operation, each node collects EEG data and wirelessly transmits it to the designated sink node, which aggregates data from multiple nodes, applies necessary synchronization corrections, and forward the data stream to the PC via USB for real-time processing. To maintain consistent timing across nodes, EEG-Linx includes a synchronization mechanism that compensates for clock drift and ensures temporal alignment. The implementation details of this protocol are discussed later in Section III-C.

A. Data Acquisition and Management

The nRF52833 microcontroller's SPI Controller interfaces with the ADS1299 to retrieve high-resolution EEG data. The SPI Controller is paired with the direct memory access (DMA) module, which automatically transfers the retrieved data to a memory buffer, minimizing CPU load and conserving power. The firmware utilizes the built-in programmable peripheral interconnect (PPI) to enable fully hardware-driven data acquisition: the ADS1299 DRDY signal directly triggers SPI communication via PPI, and then, the DMA module immediately transfers the EEG samples into memory without CPU intervention.

To ensure uninterrupted data flow, a ring buffer is employed as an intermediary storage layer between acquisition and transmission, preventing data loss when the radio module is occupied. As transient memory storage, the end-to-end time from DRDY assertion to memory storage is determined by the SPI clock rate, with a 1-MHz SPI clock completing the transfer within approximately 200 μs. Given the 4-ms intersample interval at a 250-Hz sampling rate, this duration is minimal relative to the overall acquisition process. In addition, each EEG data packet includes a high-precision timestamp, which enables accurate temporal alignment during postprocessing.

B. Wireless Data Transmission

The MCU module within the nRF52833 handles the wireless transmission of EEG data to one of the nodes, acting as a data sink. By separating data acquisition from transmission tasks, the firmware allows asynchronous data transmission, ensuring uninterrupted EEG data collection. Nodes can communicate with the data sink node or directly with each other, enabling a flexible and adaptive network for real-time monitoring across multiple locations. The underlying UDP-like communication protocol is unacknowledged and has low-overhead, resulting in very low transmission latencies, suitable for real-time EEG processing.

C. Synchronization Protocol

Synchronous sampling between the different EEG channels is crucial to facilitate multichannel signal processing methods or to perform a signal coherence analysis across the different channels. Unlike conventional EEG systems that rely on a single device with a shared clock, our distributed WESN platform consists of multiple independent wireless sensor nodes, each operating with its own local oscillator. Achieving synchronized recording in such a decentralized system is nontrivial, as slight variations in oscillator precision cause the clocks across different nodes to drift over time, leading to potential data misalignment, thereby blocking the use of advanced EEG signal processing algorithms that rely on signal coherence (e.g., independent component analysis [39], spatial filtering [40], and multichannel Wiener filtering [41]). To address these challenges, our system employs a protocol akin to the precision time protocol (PTP) to dynamically and adaptively estimate the offsets and drifts between the node's clocks [42]. The phase drift correction is implemented at the data sink node, which receives timestamped EEG data from each sensor node and continuously analyzes the relative clock differences. By comparing timestamps across nodes, the data sink estimates the drift rate and applies incremental corrections to maintain the temporal alignment of overextended recording sessions. Despite this real-time synchronization, minor residual misalignments may still exist due to subsample deviations between nodes. To achieve a higher degree of precision, the recorded data undergo additional refinement using interpolation techniques. A sinc-based interpolation approach is employed to resample each node's data onto a common

Authorized licensed use limited to: KU Leuven University Library. Downloaded on January 23,2026 at 12:16:53 UTC from IEEE Xplore. Restrictions apply.

reference timeline, which ensures all signals remain precisely aligned at the subsample level. This adaptive approach incrementally compensates for drift, achieving continuous temporal alignment across nodes even overextended periods, without requiring a centralized or shared clock.

D. USB Interface

The firmware integrates a USB interface to support data transmission, command execution, and firmware updates, offering a reliable wired alternative to wireless communication when necessary. This interface enables the EEG sensor node to connect directly to a computer for efficient data transfer and analysis. In addition, the USB interface facilitates programming and bootloader functionalities, allowing firmware updates to be applied directly over USB. This setup streamlines firmware maintenance without requiring additional hardware, enhancing the platform's adaptability.

IV. Experimental Validation

To evaluate the functionality of our EEG-Linx WESN platform, we performed validation experiments to assess: 1) its ability to maintain synchronization between nodes; 2) the impact of different hardware configurations on the signal quality; and 3) the reliability of the system in detecting neural responses.

A. Synchronization Validation

To evaluate the synchronization capability and residual internode signal drift, we conducted an experiment using a star topology. In this setup, a signal generator produced a 10-μV, 10-Hz input signal, which was added as a synthetic EEG input to three sensor nodes (Nodes 2–4). During a continuous recording period of 2 h, these three nodes amplify and digitize the sine wave signal using the ADS1299 chip and then wirelessly transmit the recorded data to a central node (Node 1). Node 1 collects the data and forwards it to a PC via the USB interface for further analysis.

Using a sliding window of 1 s, we tracked the phase differences in the 10-Hz component of the discrete Fourier transforms between all three signals. Fig. 4 shows the phase difference trajectories between Nodes 2 and 3, Nodes 2 and 4, and Nodes 3 and 4. Gradual phase differences over time indicate a drift due to slight discrepancies in each node's oscillator. With a 50-ppm precision of the oscillator at 2.048 MHz, the theoretical maximum phase drift rate is approximately 2.57×10^3 rad/s. The observed phase drift slopes for each pair of nodes (annotated in Fig. 4) show that the drift remains within this expected range.

After applying our synchronization protocol, the phase drift between nodes was significantly reduced, with near-zero slopes in the phase difference plots shown in Fig. 5. This indicates that the protocol effectively maintained a stable, synchronized data stream across the network throughout the 2-h recording period, supporting real-time alignment and accurate multichannel EEG monitoring. Though this experiment used a star topology, the synchronization method is adaptable and can be extended to other network configurations as needed.

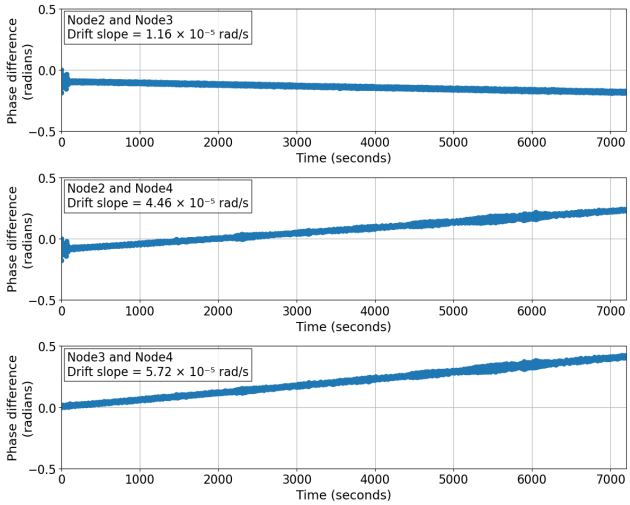


Fig. 4. Phase differences between nodes without synchronization protocol.

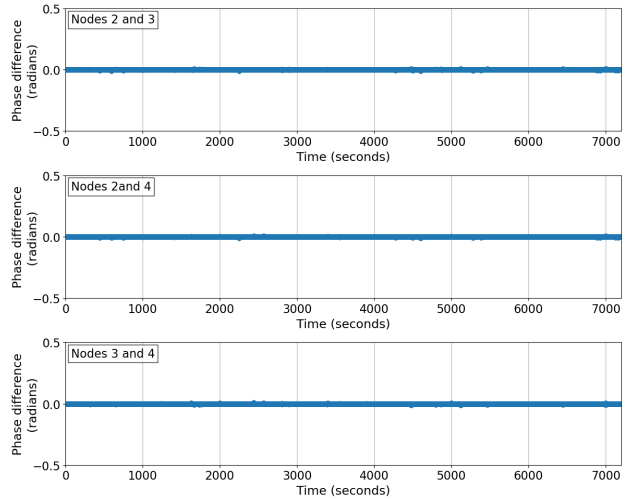


Fig. 5. Phase differences between nodes with synchronization protocol.

B. Steady-State Visually Evoked Potentials

A steady-state visually evoked potential (SSVEP) is a brain response elicited by a periodic visual stimulus such as a screen that flickers at a specific frequency. When exposed to such a repetitive flickering stimulus, the brain generates a consistent response at the same frequency, which can be detected in EEG signals that are measured near the visual cortex.

Due to their robustness and structured signal characteristics, SSVEPs are widely utilized in BCI systems [43]. In this experiment, we employed SSVEPs to validate the EEG recording performance using one single EEG-Linx node, focusing on transmission methods, DRL configurations, and electrode spacing.

We used standard wet Ag/AgCl cup electrodes with Super-Visc gel, secured to the scalp using tape. This choice was made because cup electrodes are compact and allow flexible placement. The sensor has also been successfully tested with adhesive pregelled electrodes from various vendors, demonstrating its adaptability to different electrode types. To improve

Authorized licensed use limited to: KU Leuven University Library. Downloaded on January 23,2026 at 12:16:53 UTC from IEEE Xplore. Restrictions apply.

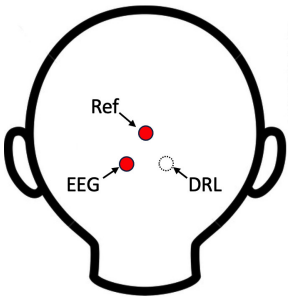
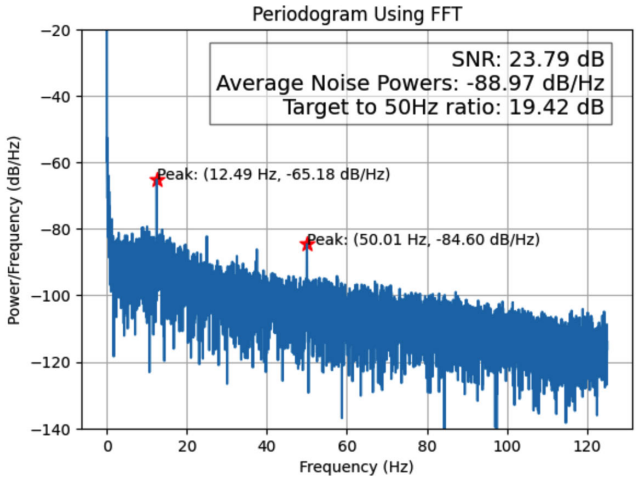


Fig. 6. Positions for the SSVEP montage.

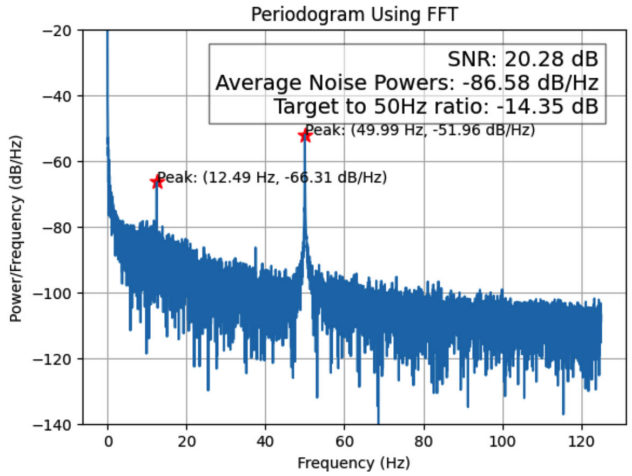
the contact between the electrode and the skin, the skin was first prepared using Nuprep gel to remove dead skin layers and oil. We verified that the impedance was $\leq$10 kΩ for each electrode before starting the measurement. The electrodes were positioned over the visual cortex area of the scalp, where SSVEP signals are most prominent [44]. The electrodes were spaced 3 cm apart. This spacing was chosen to maintain a compact design while enabling effective signal acquisition. Based on the extended 10–20 system [45], we used a bipolar montage over the visual cortex, where the active signal electrode was positioned between O1 and Oz and the reference electrode between POz and Oz. For those settings where we also used an additional DRL electrode, it was positioned between O2 and Oz. These positions are illustrated in Fig. 6. The subject was seated 0.5 m away from an LCD screen measuring 31.26 $\times$ 22.12 cm, which showed a flickering visual stimulus with a flickering frequency of 12.5 Hz. To ensure the evaluation reflects real-world conditions, all measurements were conducted in a standard office environment without electromagnetic shielding and using nonshielded cables. Continuous EEG data were recorded for one minute in each condition.

1) Wireless Versus Wired: We compared the effects of wireless and wired (USB) transmission on signal quality, using the resistor-based DRL setup with a 3-cm electrode spacing (USB transmission corresponds to a setting where an EEG sensor is connected to a PC with a cable, bypassing the wireless transmission). For each setup, the signal-to-noise ratio (SNR) was calculated as the ratio of the power at the target frequency (12.5 Hz) to the average noise power between 5 and 20 Hz. Fig. 7(a) and (b) shows the periodograms for EEG data transmitted wirelessly and via USB, respectively. In the wireless setting, the target 12.5-Hz signal is recorded with an SNR of 23.79 dB compared to the wired setting, where the SNR was 20.28 dB. Furthermore, in the wireless setting, the harmonics of the neural response at 25 and 37.5 Hz are also clearly visible, while in the wired setting, these are much harder to distinguish. Finally, the wireless transmission effectively reduces the interference at the 50-Hz power line frequency and results in lower overall background noise compared to the wired setting. This further demonstrates the advantages of avoiding wired connections in reducing interference and maintaining signal clarity.

2) Bias Resistor Validation: To evaluate the effect of different DRL configurations on the stability of the recorded EEG signals, we conducted SSVEP measurements for each



(a)



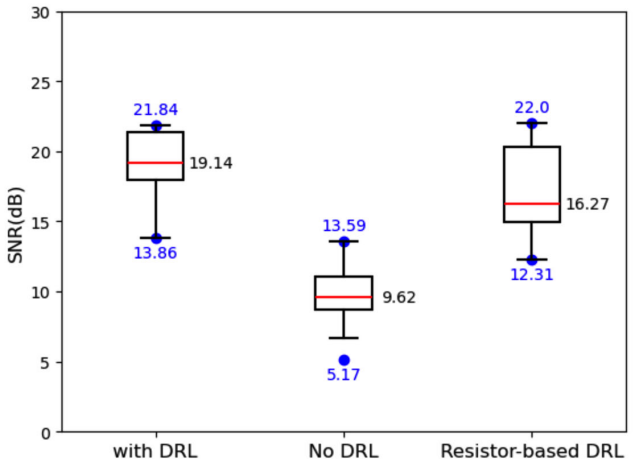
(b)

Fig. 7. SSVEP signal quality comparison: wireless versus wired. (a) Periodogram of SSVEP response with wireless transmission. (b) Periodogram of SSVEP response with wired transmission.

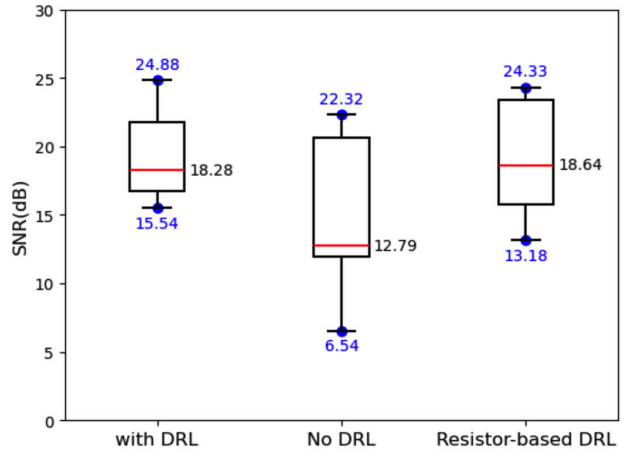
configuration over three separate days, with three 1-min recordings per day, resulting in nine data points per configuration. The experiment contains three different configurations: a conventional DRL with an additional bias electrode attached to the scalp, our resistor-based DRL configuration, and a setup without any DRL, all using the same electrode spacing of 3 cm. For each setup, we calculated the SNR as the power at the target frequency (12.5 Hz) relative to the average noise power between 5 and 20 Hz. Fig. 8(a) shows the SNR results for the wired setup, while Fig. 8(b) displays the results for the wireless setup.

In the wired (USB) configuration, the "no DRL" setup exhibited the highest variability, likely due to power line interference introduced by the USB connection, which degraded signal stability. The conventional DRL setup provided the most stable signal under this configuration, demonstrating effective suppression of the 50-Hz power line interference. The resistor-based DRL configuration, while not as stable as the conventional DRL setup, still achieved reliable performance, confirming its ability to reduce interference while simplifying the hardware setup.

Authorized licensed use limited to: KU Leuven University Library. Downloaded on January 23,2026 at 12:16:53 UTC from IEEE Xplore. Restrictions apply.



(a)



(b)

Fig. 8. Different DRL topologies for SSVEP measurement. (a) Wired (USB) setup. (b) Wireless setup.

In the wireless setup, shown in Fig. 8(b), the "no DRL" configuration showed improved stability compared to the same configuration in a wired setup, as the wireless communication reduced exposure to the power line noise. The conventional DRL setup once again demonstrated the best performance in terms of stability and SNR. Meanwhile, the resistor-based DRL setup also performed effectively in the wireless configuration, maintaining a stable signal without the need for an additional body electrode.

These results indicate that the conventional DRL setup provides optimal stability and SNR. The resistor-based configuration effectively stabilizes signals within the amplifier range while reducing the number of required electrodes. Notably, EEG-Linx remains compatible with both configurations, allowing researchers to enable a conventional DRL setup if needed, depending on experimental requirements.

3) Comparison With Commercial System: To compare the performance of EEG-Linx with a commercial EEG system, we recorded SSVEPs using both our sensor node and the mBrainTrain Smarting device, a device commonly used in BCI research [46]. Both devices receive the same input signal via a split cable connected to the same electrodes

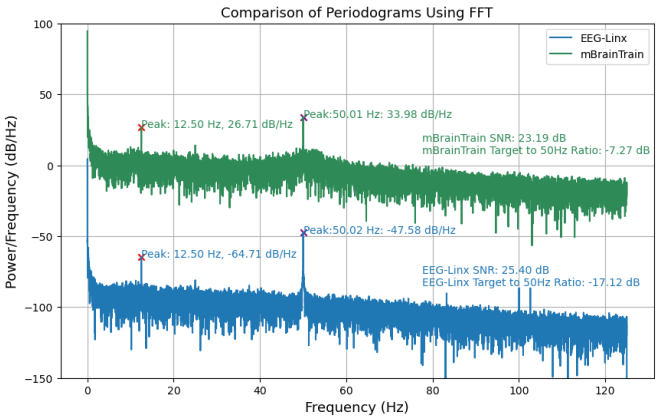


Fig. 9. EEG periodogram for mBrainTrain (top) and EEG-Linx (bottom).

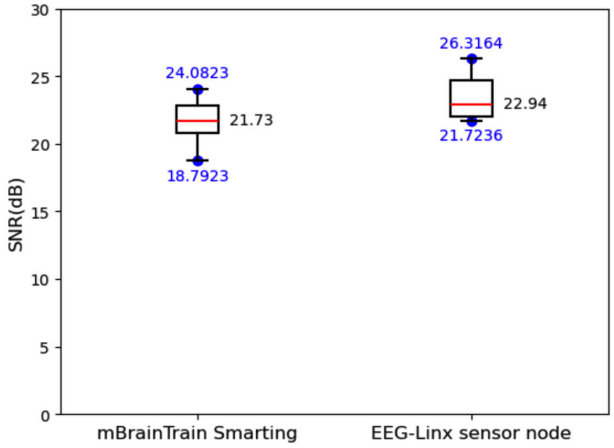


Fig. 10. Comparison of SNR of mBrainTrain Smarting and EEG-Linx sensor node for SSVEP measurement.

for consistency. Our sensor node employed two electrodes, with biasing applied through resistors, while the mBrainTrain used three electrodes, including a dedicated DRL electrode placed on the earlobe for biasing.

We repeated the experiment eight times, each with a 1-min recording session. Fig. 9 presents an overlay plot of the EEG spectrum recorded by both devices during the same recording session, illustrating the SSVEP response captured by our EEG-Linx sensor node and the mBrainTrain Smarting as an example. This comparison shows that both systems recorded similar signal spectra under identical conditions, presenting their consistency and reliability alongside a commercial device.

Furthermore, as shown in Fig. 10, a box plot comparison of SNR values indicates that our EEG-Linx sensor node achieved a slightly higher SNR on average than the mBrainTrain Smarting, despite removing the DRL electrode. This result shows the effectiveness of our platform, achieving reliable EEG signal acquisition with a simplified resistor-based biasing approach.

C. Auditory Steady-State Responses

To further validate the multinode EEG acquisition capability of EEG-Linx, we conducted an auditory steady-state response (ASSR) experiment using two EEG-Linx sensor nodes, without any wires between them. Each node recorded four EEG

Authorized licensed use limited to: KU Leuven University Library. Downloaded on January 23,2026 at 12:16:53 UTC from IEEE Xplore. Restrictions apply.

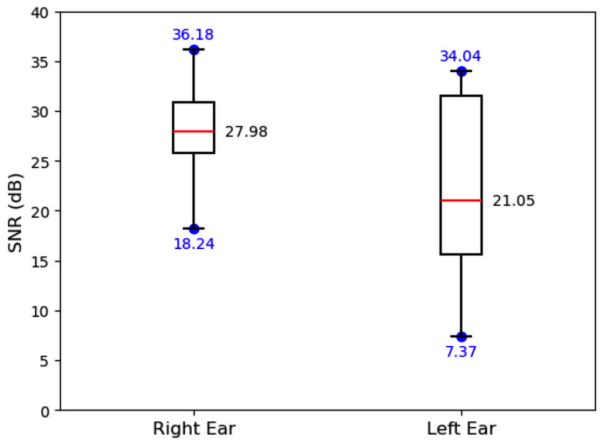


Fig. 11. SNR of left and right ear.

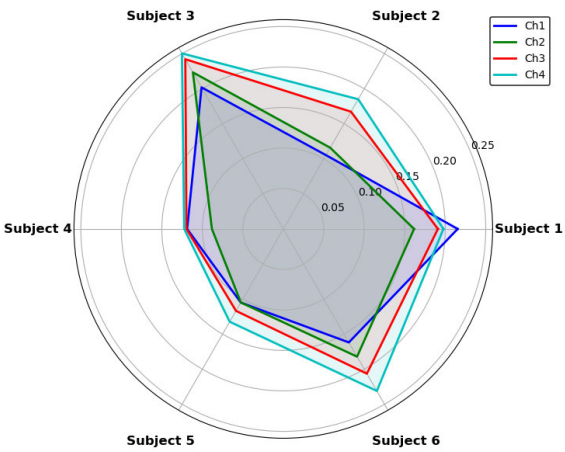


Fig. 12. Radar chart of absolute phase differences between bilateral EEG channel pairs.

channels positioned behind the left and right ears to evaluate internode synchronization and signal quality. The reference electrode for each node was placed on the ipsilateral earlobe, while the recording electrodes were evenly distributed behind the ear. Electrodes were secured using medical tape, and skin preparation followed the same protocol as in the SSVEP experiment. During the experiment, participants were presented with binaural broadband compensated envelope (CE) chirp stimuli, fully amplitude modulated at 40 Hz [47]. The auditory stimuli were delivered through in ear wired headphones at a sampling rate of 48 kHz and adjusted to a comfortable listening level for each subject.

To evaluate EEG signal quality, we computed the SNR for each of the four channels per node and averaged them for each trial (3 min per trial). A total of six subjects participated in the experiment, each completing three trials, resulting in 18 SNR measurements per ear across all participants. Fig. 11 presents a box plot of SNR values, which illustrates the distribution across all trials, all channels, and all subjects for the left and right ears. The results confirm that both nodes provided sufficiently clear signals for reliable EEG acquisition.

To evaluate the synchronization accuracy of the EEG-Linx nodes, the binaural phase difference at 40 Hz between two channels at different ears was computed across four EEG channel pairs. The phase difference was calculated using a 1-s sliding window with 50% overlap. The EEG signals from the left and right ear sensor nodes were time-aligned based on their respective timestamps using the synchronization protocol explained in Section III-C. The reported phase differences represent the average absolute values across all windows. Fig. 12 presents the phase difference results across the six subjects for four-channel pairs, showing that all channel pairs exhibit small phase differences, with values ranging approximately between 0.1 and 0.25 rad. The fact that they are not exactly 0 is due to inherent time delays between ASSR responses in different brain locations, as well as stochastic effects due to phase noise from background EEG (i.e., neural activity not related to the ASSR). However, the fact that they are so small (and within the expected range) implies that the EEG signals from both ears are properly aligned in time. For a more fine-grained assessment of synchronization across nodes, we refer to the experiment in Section IV-A, as this cannot be shown using EEG signals alone due to their low SNR and variability.

V. Conclusion

In this study, we introduced EEG-Linx, a modular WESN-based platform optimized for flexible and discreet multichannel EEG monitoring. Through miniaturized sensor nodes and a resistor-based biasing method, EEG-Linx allows for discreet form factors while maintaining reliable signal quality and large scalp coverage. A custom synchronization protocol was implemented to address the challenge of oscillator drift, enabling stable internode signal alignment during prolonged recordings. Validation experiments demonstrated that EEG-Linx achieves a high SNR in SSVEP recordings, which is comparable to DRL-equipped commercial systems despite its reduced hardware footprint. This performance, combined with its scalability and flexibility, establishes EEG-Linx as a reliable solution for portable EEG applications.

Acknowledgment

Views and opinions expressed are, however, those of the author(s) only and do not necessarily reflect those of European Union or ERC. Neither European Union nor the granting authority can be held responsible for them.

References

[1] H. Zhang et al., "The applied principles of EEG analysis methods in neuroscience and clinical neurology," *Mil. Med. Res.*, vol. 10, no. 1, p. 67, Dec. 2023, doi: 10.1186/s40779-023-00502-7.

[2] Z. Lian, T. Xu, Z. Yuan, J. Li, N. Thakor, and H. Wang, "Driving fatigue detection based on hybrid electroencephalography and eye tracking," *IEEE J. Biomed. Health Informat.*, vol. 28, no. 11, pp. 6568–6580, Nov. 2024. [Online]. Available: https://ieeexplore.ieee.org/abstract/document/10643252/

[3] I. C. Zibrandtsen, P. Kidmose, C. B. Christensen, and T. W. Kjaer, "Ear-EEG detects ictal and interictal abnormalities in focal and generalized epilepsy—A comparison with scalp EEG monitoring," *Clin. Neurophysiol.*, vol. 128, no. 12, pp. 2454–2461, Dec. 2017.

[4] L. Swinnen et al., "Accurate detection of typical absence seizures in adults and children using a two-channel electroencephalographic wearable behind the ears," *Epilepsia*, vol. 62, no. 11, pp. 2741–2752, Nov. 2021, doi: 10.1111/epi.17061.

Authorized licensed use limited to: KU Leuven University Library. Downloaded on January 23,2026 at 12:16:53 UTC from IEEE Xplore. Restrictions apply.

[5] E. R. M. Heremans, N. Seedat, B. Buyse, D. Testelmans, M. Van Der Schaar, and M. De Vos, "U-PASS: An uncertainty-guided deep learning pipeline for automated sleep staging," *Comput. Biol. Med.*, vol. 171, Mar. 2024, Art. no. 108205.

[6] E. R. M. Heremans, H. Phan, P. Borzée, B. Buyse, D. Testelmans, and M. De Vos, "From unsupervised to semi-supervised adversarial domain adaptation in electroencephalography-based sleep staging," *J. Neural Eng.*, vol. 19, no. 3, Jun. 2022, Art. no. 036044.

[7] E. Kutafina et al., "Tracking of mental workload with a mobile EEG sensor," *Sensors*, vol. 21, no. 15, p. 5205, Jul. 2021.

[8] S. Charbonnier, R. N. Roy, S. Bonnet, and A. Campagne, "EEG index for control operators' mental fatigue monitoring using interactions between brain regions," *Expert Syst. Appl.*, vol. 52, pp. 91–98, Jun. 2016.

[9] S. Debener, F. Minow, R. Emkes, K. Gandras, and M. De Vos, "How about taking a low-cost, small, and wireless EEG for a walk?" *Psychophysiology*, vol. 49, no. 11, pp. 1617–1621, Nov. 2012, doi: 10.1111/j.1469-8986.2012.01471.x.

[10] S. Geirnaert et al., "Electroencephalography-based auditory attention decoding: Toward neurosteered hearing devices," *IEEE Signal Process. Mag.*, vol. 38, no. 4, pp. 89–102, Jul. 2021.

[11] G. Niso, E. Romero, J. T. Moreau, A. Araujo, and L. R. Krol, "Wireless EEG: A survey of systems and studies," *NeuroImage*, vol. 269, Apr. 2023, Art. no. 119774, doi: 10.1016/j.neuroimage.2022.119774.

[12] R. Portillo-Lara, B. Tahirbegi, C. A. R. Chapman, J. A. Goding, and R. A. Green, "Mind the gap: State-of-the-art technologies and applications for EEG-based brain–computer interfaces," *APL Bioengineering*, vol. 5, no. 3, Sep. 2021, Art. no. 031507. [Online]. Available: https://pubs.aip.org/aip/apb/article/5/3/031507/149807

[13] K. B. Mikkelsen, S. L. Kappel, D. P. Mandic, and P. Kidmose, "EEG recorded from the ear: Characterizing the ear-EEG method," *Frontiers Neurosci.*, vol. 9, p. 438, Nov. 2015.

[14] Y. R. Tabar, K. B. Mikkelsen, M. L. Rank, M. C. Hemmsen, M. Otto, and P. Kidmose, "Ear-EEG for sleep assessment: A comparison with actigraphy and PSG," *Sleep Breathing*, vol. 25, no. 3, pp. 1693–1705, Sep. 2021, doi: 10.1007/s11325-020-02248-1.

[15] S. Debener, R. Emkes, M. De Vos, and M. Bleichner, "Unobtrusive ambulatory EEG using a smartphone and flexible printed electrodes around the ear," *Sci. Rep.*, vol. 5, no. 1, p. 16743, Nov. 2015.

[16] A. Bertrand, "Distributed signal processing for wireless EEG sensor networks," *IEEE Trans. Neural Syst. Rehabil. Eng.*, vol. 23, no. 6, pp. 923–935, Nov. 2015, doi: 10.1109/TNSRE.2015.2418351.

[17] T. Strypsteen and A. Bertrand, "Bandwidth-efficient distributed neural network architectures with application to neuro-sensor networks," *IEEE J. Biomed. Health Informat.*, vol. 27, no. 2, pp. 933–943, Feb. 2023.

[18] B. Somers and A. Bertrand, "Removal of eye blink artifacts in wireless EEG sensor networks using reduced-bandwidth canonical correlation analysis," *J. Neural Eng.*, vol. 13, no. 6, Dec. 2016, Art. no. 066008.

[19] A. M. Narayanan and A. Bertrand, "Analysis of miniaturization effects and channel selection strategies for EEG sensor networks with application to auditory attention detection," *IEEE Trans. Biomed. Eng.*, vol. 67, no. 1, pp. 234–244, Jan. 2020, doi: 10.1109/TBME.2019.2911728.

[20] A. M. Narayanan, P. Patrinos, and A. Bertrand, "Optimal versus approximate channel selection methods for EEG decoding with application to topology-constrained neuro-sensor networks," *IEEE Trans. Neural Syst. Rehabil. Eng.*, vol. 29, pp. 92–102, 2021.

[21] A. Mundanad Narayanan, R. Zink, and A. Bertrand, "EEG miniaturization limits for stimulus decoding with EEG sensor networks," *J. Neural Eng.*, vol. 18, no. 5, Oct. 2021, Art. no. 056042, doi: 10.1088/1741-2552/ac2629.

[22] J. Dan, M. T. Foged, B. Vandendriessche, W. Van Paesschen, and A. Bertrand, "Sensor selection and miniaturization limits for detection of interictal epileptiform discharges with wearable EEG," *J. Neural Eng.*, vol. 20, no. 1, Feb. 2023, Art. no. 016045, doi: 10.1088/1741-2552/acb231.

[23] F. Battaglia, G. Gugliandolo, G. Campobello, and N. Donato, "EEG-over-BLE: A novel low-power architecture for multi-channel EEG monitoring systems," in *Proc. IEEE Int. Symp. Meas. Netw. (MN)*, Jul. 2022, pp. 1–6, doi: 10.1109/MN55117.2022.9887765.

[24] J. Lee et al., "A 0.8-V 82.9-μ W in-ear BCI controller IC with 8.8 PEF EEG instrumentation amplifier and wireless BAN transceiver," *IEEE J. Solid-State Circuits*, vol. 54, no. 4, pp. 1185–1195, Apr. 2019.

[25] L. O. H. Z. Toresano, S. K. Wijaya, Prawito, A. Sudarmaji, and C. Badri, "Data acquisition system of 16-channel EEG based on ATSAM3X8E ARM cortex-M3 32-bit microcontroller and ADS1299," in *Proc. AIP Conf.*, Aug. 2017, Paper 030149. [Online]. Available: https://pubs.aip.org/aip/acp/article-abstract/1862/1/030149/649943

[26] S. Patki et al., "Wireless EEG system with real time impedance monitoring and active electrodes," in *Proc. IEEE Biomed. Circuits Syst. Conf. (BioCAS)*, Nov. 2012, pp. 108–111, doi: 10.1109/BIOCAS.2012.6418408.

[27] M. Sawan et al., "Wireless recording systems: From noninvasive EEG-NIRS to invasive EEG devices," *IEEE Trans. Biomed. Circuits Syst.*, vol. 7, no. 2, pp. 186–195, Apr. 2013, doi: 10.1109/TBCAS.2013.2255595.

[28] U. Ghoshdastider, R. Viga, and M. Kraft, "Wireless time synchronization of a collaborative brain–computer-interface using Bluetooth low energy," in *Proc. IEEE SENSORS*, Nov. 2014, pp. 2250–2254, doi: 10.1109/ICSENS.2014.6985489.

[29] T. T. Vo, N. P. Nguyen, and T. Vo Van, "WEEGEE: Wireless 8-channel EEG recording device," in *Proc. 6th Int. Conf. Develop. Biomed. Eng. Vietnam (BME6)*, vol. 63. Singapore: Springer, 2018, pp. 621–625, doi: 10.1007/978-981-10-4361-1_106.

[30] *ADS1299-xLow-Noise,4-,6-,8-Channel,24-Bit, Analog-to-Digital Converter for EEG and Bio Potential Measurements*, Texas Instruments, Dallas, TX, USA, 2017.

[31] A. M. Narayanan and A. Bertrand, "The effect of miniaturization and galvanic separation of EEG sensor devices in an auditory attention detection task," in *Proc. 40th Annu. Int. Conf. IEEE Eng. Med. Biol. Soc. (EMBC)*, Jul. 2018, pp. 77–80, doi: 10.1109/EMBC.2018.8512212.

[32] M. G. Bleichner et al., "Exploring miniaturized EEG electrodes for brain–computer interfaces. An EEG you do not see?" *Physiological Rep.*, vol. 3, no. 4, Apr. 2015, Art. no. e12362, doi: 10.14814/phy2.12362.

[33] V. Mihajlovic, B. Grundlehner, R. Vullers, and J. Penders, "Wearable, wireless EEG solutions in daily life applications: What are we missing?" *IEEE J. Biomed. Health Informat.*, vol. 19, no. 1, pp. 6–21, Jan. 2015, doi: 10.1109/JBHI.2014.2328317.

[34] M. F. Chimene and R. Pallas-Areny, "A comprehensive model for power line interference in biopotential measurements," *IEEE Trans. Instrum. Meas.*, vol. 49, no. 3, pp. 535–540, Jun. 2000.

[35] M. D. R. Perin, R. W. Porto, A. Z. Neto, and M. M. Spindola, "EOG analog front-end for human machine interface," in *Proc. IEEE Int. Instrum. Meas. Technol. Conf. (I2MTC)*, May 2017, pp. 1–6. Accessed: Aug. 27, 2024. [Online]. Available: https://ieeexplore.ieee.org/abstract/document/7969711/

[36] T. Instruments. (Apr. 2012). *Improving Common-mode Rejection Using the Right-leg Drive Amplifier*. [Online]. Available: https://www.ti.com/lit/an/sbaa188/sbaa188.pdf

[37] E. M. Spinelli and M. A. Mayosky, "Two-electrode biopotential measurements: Power line interference analysis," *IEEE Trans. Biomed. Eng.*, vol. 52, no. 8, pp. 1436–1442, Aug. 2005.

[38] R. Pallas-Areny, "On the reduction of interference due to common mode voltage in two-electrode biopotential amplifiers," *IEEE Trans. Biomed. Eng.*, vol. BME-33, no. 11, pp. 1043–1046, Nov. 1986.

[39] J. Onton, M. Westerfield, J. Townsend, and S. Makeig, "Imaging human EEG dynamics using independent component analysis," *Neurosci. Biobehavioral Rev.*, vol. 30, no. 6, pp. 808–822, Jan. 2006.

[40] B. Blankertz, R. Tomioka, S. Lemm, M. Kawanabe, and K.-R. Müller, "Optimizing spatial filters for robust EEG single-trial analysis," *IEEE Signal Process. Mag.*, vol. 25, no. 1, pp. 41–56, Jan. 2008.

[41] B. Somers, T. Francart, and A. Bertrand, "A generic EEG artifact removal algorithm based on the multi-channel Wiener filter," *J. Neural Eng.*, vol. 15, no. 3, Jun. 2018, Art. no. 036007.

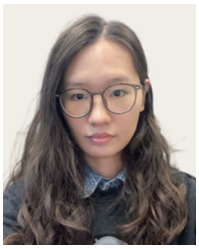
[42] *IEEE Standard for a Precision Clock Synchronization Protocol for Networked Measurement and Control Systems*, IEEE Standard 1588. [Online]. Available: https://standards.ieee.org/ieee/1588/6825/

[43] Y. Punsawad and Y. Wongsawat. (2011). *Enhancement of SSVEP-based BCI System Via SSAEP During Eye Fatigue Period*. [Online]. Available: https://www.academia.edu/download/82906960/APSIPA258.pdf

[44] F. Di Russo et al., "Spatiotemporal analysis of the cortical sources of the steady-state visual evoked potential," *Human Brain Mapping*, vol. 28, no. 4, pp. 323–334, Apr. 2007, doi: 10.1002/hbm.20276.

Authorized licensed use limited to: KU Leuven University Library. Downloaded on January 23,2026 at 12:16:53 UTC from IEEE Xplore. Restrictions apply.

[45] R. W. Homan, J. Herman, and P. Purdy, "Cerebral location of international 10–20 system electrode placement," *Electroencephalogr. Clin. Neurophysiology*, vol. 66, no. 4, pp. 376–382, Apr. 1987.
[46] mBrainTrain. *Smarting Wireless EEG*. Accessed: Apr. 24, 2025. [Online]. Available: https://mbraintrain.com/smarting-wireless-eeg/
[47] C. B. Christensen, T. Lunner, J. M. Harte, M. L. Rank, and P. Kidmose, "Chirp-evoked auditory steady-state response: The effect of repetition rate," *IEEE Trans. Biomed. Eng.*, vol. 69, no. 2, pp. 689–699, Feb. 2022.



Ruochen Ding received the B.Eng. degree from the Polytech Nice-Sophia, Biot, France, in 2020, and the Ph.D. degree at Université Côte d'Azur, Nice, France, in 2023, where she focused on RF circuits for low-power wireless communication.

She is currently a Postdoctoral Researcher at the Department of Electrical Engineering (ESAT), KU Leuven, Belgium, working within the research groups of Prof. Alexander Bertrand and Prof. Michael Kraft. Her research in the NeuroSense project focuses on interface circuits for physiological recordings using wearable EEG sensor nodes.



Charles Hovine received the M.Sc. degree in electrical engineering from UCLouvain, Ottignies-Louvain-la-Neuve, Belgium, in 2015, and the Ph.D. degree from the Electrical Engineering Department, KU Leuven, Belgium, in 2024.

From 2015 to 2018, he worked as a Research and Development Engineer with the Fixed Networks Division, Nokia, Antwerp, Belgium. He was part of the research group with KU Leuven led by Prof. Alexander Bertrand. His research focused on bandwith-efficient distributed signal processing algorithms.

Dr. Hovine was a recipient of IEEE EUSIPCO 2021 Best Student Paper Award.

Piet Callemeyn was born in Roeselare, Belgium in 1987. He received the M.Sc. degree in electrical engineering from KU Leuven, Leuven, Belgium, in 2010, and the Ph.D. degree in electrical engineering from KU Leuven, MICAS research group, in 2015. His Ph.D. thesis is entitled "Fully-Integrated CMOS DC-AC converters."

In 2017, he founded the company Sentineo, based in Leuven, focusing on custom embedded hardware design of ultra-low power connected systems.

Dr. Callemeyn is the co-recipient of the 2012 Texas Instruments Engibous Prize for Innovation in Analog Design in the EMEA region.



Michael Kraft (Member, IEEE) received the Dipl.-Ing. degree in electrical and electronics engineering from the Friedrich Alexander Universität Erlangen-Nürnberg, Erlangen, Germany, in 1993, and the Ph.D. degree from Coventry University, Coventry, U.K., in 1997, on the development of an MEMS accelerometer.

He has been a Full Professor of microsystem and nanosystem at the Department of Electrical Engineering, KU Leuven, Leuven, Belgium, since 2017. He was the Head of the Research Division Micro- and Nanosystems and the Acting Director of Leuven Institute for Micro and Nanoscale Integration (LIMNI) Leuven. He is also a Guest Professor at imec, Leuven. Before joining KU Leuven, he was a Professor at the University of Liège, Liège, Belgium, from 2015 to 2017, where he was responsible for the microsys cleanroom. From 2012 to 2014, he was at the Fraunhofer Institute for Microelectronic Circuits and Systems, Duisburg, Germany, where he was the Head of Department of Micro- and Nanosystems focusing on fully integrated microsensors and biohybrid systems. He concurrently held the W3 Professorial Chair of integrated microsystem and nanosystem at the University of Duisburg-Essen, Duisburg. From 1999 to 2012, he was a Faculty Member and a Professor of microsystem technology with the University of Southampton, Southampton, U.K. He then spent two years at Berkeley Sensors and Actuator Centre at the University of California, Berkeley, CA, USA, working on integrated MEMS gyroscopes. He has more than 25 years of experience in micro/nano fabrication techniques, microsensors and actuators and their interface circuits. He has a broad interest in MEMS and nanotechnology ranging from process development to system integration of MEMS and nanodevices. He has published over 300 peer-reviewed journal and conference publications as an author or co-author. He also contributed to four textbooks on MEMS as an author and an editor.

Dr. Kraft has served on several steering and technical committees of international conferences such as Transducers, IEEE MEMS, ISSCC, IEEE Sensors, Eurosensors, MNE and MME, as well as being an Associate Editor for IEEE SENSORS LETTER, IEEE JOURNAL OF MICROELECTROMECHANICAL SYSTEMS, *Journal of Micromechanics and Microengineering* (IOP), *Sensors* (MDPI), and the *Journal of Sensors and Sensor Systems* (AMA).



Alexander Bertrand (Senior Member, IEEE) received the Ph.D. degree in engineering sciences (electrical engineering) from KU Leuven, Leuven, Belgium, in 2011.

He is currently a Professor with the Department of Electrical Engineering, KU Leuven. His research interests include signal processing algorithm design, with a focus on (biomedical) sensor arrays such as electroencephalography, neural implants, ultrasound probes, and distributed body and neurosensor networks. He also conducts research in generic signal processing techniques, with a focus on multichannel and distributed signal processing.

Dr. Bertrand was the recipient of an ERC grant, the 2023 'Early Career Award' of the European Signal Processing Association (EURASIP), the 2012 FWO/IBM-Belgium Award, the 2013 KU Leuven Research Council Award, and several research fellowships and grants. He is currently Senior Area Editor for IEEE TRANSACTIONS ON SIGNAL PROCESSING, and was an Associate Editor for the same journal (2 terms), lead Guest Editor for *Signal Processing* (Elsevier), part of the Organizing Committee of IEEE ICASSP 2023, EUSIPCO 2025, and IEEE CAMSAP 2025, and Technical Program Committee Member for several international signal processing conferences and workshops.

Authorized licensed use limited to: KU Leuven University Library. Downloaded on January 23,2026 at 12:16:53 UTC from IEEE Xplore. Restrictions apply.